

## Tuning the interlayer of transition metal oxides for electrochemical energy storage

Veronica Augustyn<sup>a)</sup>

Department of Materials Science & Engineering, North Carolina State University, Raleigh, NC 27606

(Received 1 July 2016; accepted 29 August 2016)

Layered transition metal oxides are some of the most important materials for high energy and power density electrochemical energy storage, such as batteries and electrochemical capacitors. These oxides can efficiently store charge via intercalation of ions into the interlayer vacant sites of the bulk material. The interlayer can be tuned to modify the electrochemical environment of the intercalating species to allow improved interfacial charge transfer and/or solid-state diffusion. The ability to fine-tune the solid-state environment for energy storage is highly beneficial for the design of layered oxides for specific mechanisms, including multivalent ion intercalation. This review focuses on the benefits as well as the methods for interlayer modification of layered oxides, which include the presence of structural water, solvent cointercalation and exchange, cation exchange, polymers, and small molecules, exfoliation, and exfoliated heterostructures. These methods are an important design tool for further development of layered oxides for electrochemical energy storage applications.



Veronica Augustyn

Veronica Augustyn is an Assistant Professor of Materials Science & Engineering at North Carolina State University. She received her B.S. (2007) from the University of Arizona and Ph.D. (2013) from the University of California, Los Angeles, all in Materials Science and Engineering. From 2013 to 2015, she was a Postdoctoral Fellow at the Texas Materials Institute at the University of Texas at Austin. Her research is focused on the development and characterization of materials for electrochemical energy technologies including batteries, electrochemical capacitors, and electrolyzers. In particular, she is interested in the relationships between material structure and morphology and the resulting redox behavior and electrochemical mechanisms. In addition to her research interests, she leads an award-winning international outreach project at NC State, SciBridge, which develops renewable energy research and education collaborations between universities in east Africa and the U.S.

### I. INTRODUCTION & BACKGROUND

According to the U.S. National Air and Space Administration (NASA), the level of CO<sub>2</sub> in the atmosphere has exceeded 400 ppm, the highest it has been in over 400,000 years.<sup>1</sup> At the same time, over 1 billion people, primarily in sub-Saharan Africa and Asia, do not have access to electricity. These environmental and human development factors lead to a pressing need for grid energy storage to enable the integration of sustainable energy conversion devices, which are typically intermittent in nature. In addition, portable electronics and electric vehicles continue to proliferate and push the performance of lightweight, high volumetric energy density storage devices. For these diverse applications, electrochemical energy storage is the primary energy storage technology due to the large number of

chemistries, their scalability, and efficiency. In addition to the large application demand, the constantly evolving capability to understand phenomena at electrochemical interfaces is leading to significant improvements in the fundamental understanding of electrochemical processes. Electrochemical measurements have now been coupled with such advanced materials characterization techniques as transmission electron microscopy (TEM),<sup>2–4</sup> x-ray diffraction (XRD),<sup>5–7</sup> x-ray absorption (XAS),<sup>8,9</sup> atomic force microscopy (AFM),<sup>10–12</sup> and Raman microscopy,<sup>13–15</sup> to name just a few. This pairing has enabled *in situ* and *operando* characterization of materials for electrochemical technologies leading to advancements in the mechanistic understanding of interfacial phenomena. Lastly, advancements in materials synthesis are leading to the control of materials at the atomic scale<sup>16–18</sup> so that electrochemical energy storage electrodes can be highly tailored for diverse applications, from small sensors<sup>19,20</sup> to grid energy storage.<sup>21</sup> With this congruence of societal need, improved understanding of interfaces, and control over material

Contributing Editor: Chongmin Wang

<sup>a)</sup>Address all correspondence to this author.

e-mail: vaugust@ncsu.edu

DOI: 10.1557/jmr.2016.337

synthesis, it is no wonder that the present time is being hailed as the ‘golden age’ for electrochemistry.<sup>22</sup>

Within this dynamic research and application landscape, layered transition metal oxides are a highly important class of materials for electrochemical energy storage due to their use in lithium ion battery cathodes,<sup>23</sup> sodium ion battery cathodes,<sup>24</sup> and electrochemical capacitors.<sup>25</sup> The unique feature of these materials is the presence of an interlayer region that serves as the host for ion intercalation. The purpose of this review is to describe methods by which the interlayer of layered metal oxides can be tuned to achieve improvements in electrochemical performance or for new mechanisms of energy storage. The interlayer modifications discussed are the presence of structural water, solvent cointercalation and exchange, cation exchange, polymers, and small molecules, exfoliation, and synthesis of exfoliated metal oxide heterostructures.

## II. STRUCTURE OF LAYERED TRANSITION METAL OXIDES

The wide interlayer spacing and weak interlayer bonding of layered oxide materials allows for the intercalation of a large variety of guest species, including cations, anions, and polymers. These layered structures are built up of transition metal–oxygen clusters, with the transition metal typically in octahedral, or 6-fold, coordination by oxygen ligands.<sup>26</sup> In layered oxides, the strong interaction between the transition metal cation and the electrons of the oxygen ligand means that oxygens will bond weakly to transition metals in adjacent layers.<sup>26</sup> The octahedra are assembled into extended structures by sharing corners, edges, and rarely, faces. The critical feature of layered transition metal oxides is that the intralayer bonding is significantly stronger than the interlayer bonding. The layered oxides are typically formed by transition metals in high oxidation states—+4, +5, and +6. Figure 1 illustrates the layered

structure of several different redox-active layered oxides: (a) layered birnessite  $\text{MnO}_2$  ( $\delta\text{-MnO}_2$ ), (b) orthorhombic  $\text{V}_2\text{O}_5$ , and (c) monoclinic  $\text{WO}_3 \cdot 2\text{H}_2\text{O}$ . These represent the variety of layered structures built up from  $\text{MO}_6$  octahedra sharing edges and corners. Layered oxide structures are extremely versatile and allow for modification of both the inorganic framework (via substitutional doping<sup>27</sup> or vacancy formation)<sup>28</sup> and the interlayer; the latter is the focus of this review.

## III. MECHANISMS OF ELECTROCHEMICAL ENERGY STORAGE IN LAYERED TRANSITION METAL OXIDES

The development of high energy density electrochemical storage is in large part due to the properties of layered transition metal oxides. These include high ionic and electronic conductivity, capability of undergoing redox reactions, and the availability of interlayer sites for the intercalation of cations from the electrolyte. In general, when a layered metal oxide is placed in contact with an electrolyte, several different mechanisms are possible. In order of increased capacity and structural disorder, these are: (i) double-layer capacitance,<sup>29</sup> (ii) pseudocapacitance,<sup>25</sup> (iii) intercalation,<sup>30</sup> (iv) decomposition,<sup>31</sup> and (v) conversion,<sup>32</sup> as illustrated in Fig. 2. Double-layer capacitance is the only mechanism that is purely electrostatic and therefore does not contain a charge transfer step.<sup>33</sup> As a result, this mechanism provides lifetimes of over 1 million cycles, which are orders of magnitude greater than with mechanisms that involve a redox process. The highest capacitances of  $\sim 150 \text{ F/g}$  are obtained with high surface area ( $>1000 \text{ m}^2/\text{g}$ ) carbon materials.<sup>34</sup> Two different types of Faradaic capacitance (pseudocapacitance) can occur in transition metal oxides: redox pseudocapacitance and intercalation pseudocapacitance.<sup>35</sup> Redox pseudocapacitance occurs due to surface or near-surface redox reactions; materials that exhibit this

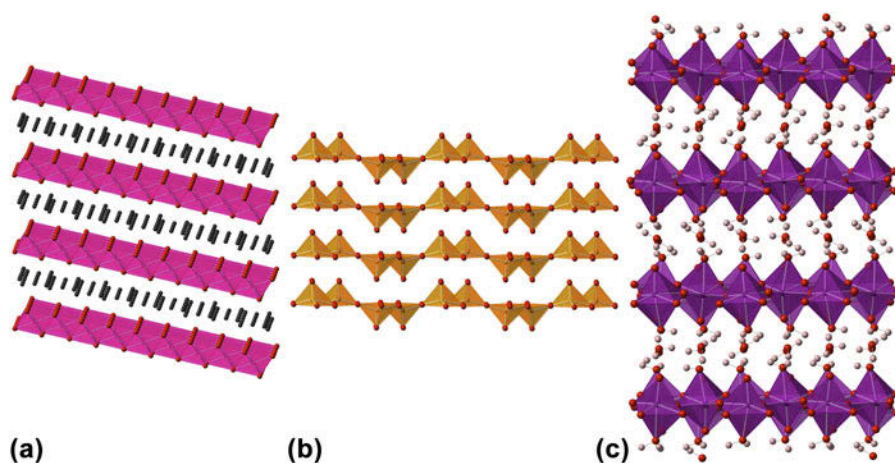


FIG. 1. Examples of layered transition metal oxides for electrochemical energy storage: (a) birnessite ( $\delta$ )  $\text{MnO}_2$ , (b) orthorhombic  $\text{V}_2\text{O}_5$ , and (c) monoclinic  $\text{WO}_3 \cdot 2\text{H}_2\text{O}$ .

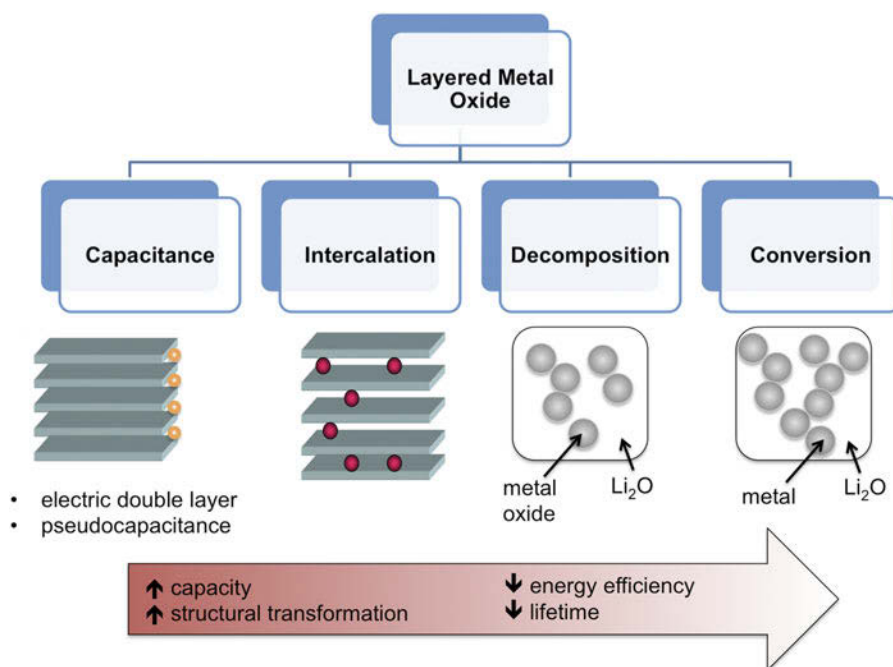
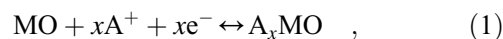


FIG. 2. Possible mechanisms of electrochemical energy storage in layered transition metal oxides. From left to right, the capacity (total amount of charge stored) increases, but so does the level of structural transformation, which results in decreasing energy efficiency and lifetime.

phenomenon include  $\text{RuO}_2 \cdot 0.5\text{H}_2\text{O}$  (Ref. 36) as well as most nanostructured transition metal oxides.<sup>37</sup> Intercalation pseudocapacitance occurs due to redox reactions at the surface as well as the bulk that are not kinetically limited by solid-state diffusion or phase transitions, as in  $\text{Nb}_2\text{O}_5$ .<sup>38</sup> When present, both pseudocapacitive mechanisms will exhibit capacitive, or surface-limited, kinetics,<sup>25</sup> with capacitance values between  $\sim 300$  and  $1000$  F/g. Intercalation reactions encompass a more general mechanism than intercalation pseudocapacitance, in that kinetics can be limited by solid-state diffusion and nucleation of a new phase can occur. Intercalation reactions provide capacities of up to  $400$  mA h/g in the case of multi-electron intercalation.<sup>39</sup> Decomposition and conversion reactions destroy the layered transition metal oxide structure during the 1st cycle, and require the nucleation of  $\text{Li}_2\text{O}$  and suboxides or metal nanoparticles.<sup>40</sup> These reactions provide the highest capacities for energy storage with metal oxides, typically  $>500$  mA h/g.<sup>32,41</sup> The reversibility and rate capability of decomposition and conversion reactions is high after the first cycle, but due to the variation in reaction pathways between the lithiation/delithiation processes, the overall energy efficiency is low (typically,  $\sim 1$  V hysteresis occurs even at low rates in oxides).<sup>42,43</sup> Despite many years of intense effort to overcome this issue by designing highly advanced electrode architectures, it has been extremely challenging to improve the energy efficiency sufficiently for application in commercial devices.<sup>44</sup>

Intercalation is the best mechanism for energy storage in metal oxides when considering the optimization of capacity, rate capability, efficiency, and lifetime. The general intercalation equation is:



where MO is a layered transition metal oxide and  $\text{A}^+$  is a cation (typically  $\text{H}^+$ ,  $\text{Li}^+$ , and  $\text{Na}^+$  but multivalent ions such as  $\text{Mg}^{2+}$  and  $\text{Al}^{3+}$  can also intercalate). As a result of the beneficial properties of intercalation, the mechanism has been successfully utilized for high energy density electrochemical energy storage in commercially-available lithium-ion and nickel-metal hydride batteries (Ni/MH).<sup>45</sup> The intercalation mechanism occurs via four primary steps (Fig. 3)<sup>46</sup>: (i) ion diffusion in the electrolyte to the electrode/electrolyte interface, (ii) surface diffusion of the ion to an intercalation site, (iii) charge transfer at the interface, and (iv) diffusion in the solid state. Each of these steps can be affected by the properties of the interlayer in layered transition metal oxides.

#### IV. BENEFITS OF INTERLAYER MODIFICATION FOR ELECTROCHEMICAL ENERGY STORAGE

Interlayer modification presents an additional level of control over the electrochemical behavior of oxides for electrochemical energy storage based on intercalation reactions. At the interface, interlayer modification of layered structures can affect the activation energy and

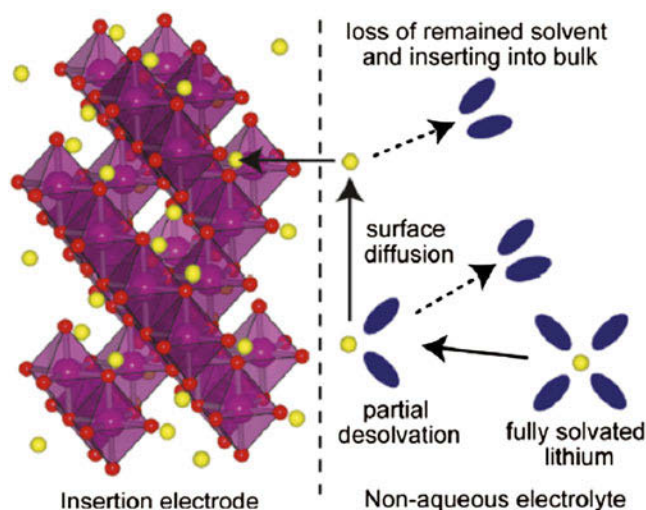


FIG. 3. The four primary steps of ion intercalation into a solid host, illustrated for  $\text{Li}^+$  insertion from a non-aqueous electrolyte. Reprinted with permission from Ref. 47. Copyright 2011 American Chemical Society.

potential for charge transfer. In the bulk, it may affect the electronic conductivity of the structure if the interlayer modification involves the intercalation of cations to form a partially reduced compound. Interlayer modification will affect the transport of the intercalating ion, and may alter the ion storage sites. In this section, the effect of interlayer modification on interfacial charge transfer and diffusion is presented in detail.

### A. Interfacial charge transfer

The charge-transfer stage is a critical step where an ion transfers from a (typically) liquid phase into a solid phase at the same time that an electron is transferred into the solid phase. When transferring from a liquid electrolyte, the ion typically needs to lose its solvation shell<sup>48</sup> and, in the case of multivalent cations, other ions.<sup>49</sup> In theoretical descriptions of charge transfer, an intermediate, transient step is assumed between the solvated stage and the intercalated stage. The difference in energy between the solvated stage and the transient stage is the activation energy for charge-transfer during intercalation ( $E_a$ ), and may be related to the charge transfer resistance ( $R_{CT}$ )<sup>48</sup>:

$$\frac{1}{R_{CT}} = A_0 \exp(-E_a/kT) \quad (2)$$

Here,  $A_0$  is a pre-exponential constant,  $k$  is the ideal gas constant, and  $T$  is the temperature. The activation energy for charge transfer has been ascribed as the energy required to desolvate the intercalating cation.<sup>48</sup> Modification of the interlayer that allows for solvent co-intercalation or partial cation solvation in the structure can thus decrease the activation energy for charge transfer.

### B. Ion transport in the interlayer

Once the ion has been intercalated, it undergoes solid-state diffusion due to the concentration gradient developed between the surface and the bulk of the material. Typically, diffusion is the rate-limiting step for ion intercalation in electrochemical energy storage<sup>50</sup> except in the case of intercalation pseudocapacitance, which is surface limited.<sup>38</sup> In most layered compounds, the ions move via interstitial vacancies in a 2D plane. In a layered oxide with a modified interlayer, the ion may diffuse via different mechanisms. For example, in a hydrated, layered structure, the ion may move via the Grotthuss mechanism responsible for rapid proton diffusion in water.<sup>51</sup> The use of interlayer solvation in multivalent ion intercalation is beneficial for screening the diffusing ion from the inorganic framework.<sup>52,53</sup>

The interlayer environment can lead to changes in the rate capability for ion intercalation due to its influence on the diffusion coefficient,  $D$ <sup>54</sup>:

$$D = p\lambda^2\nu^* \exp(-E_B/kT) \quad (3)$$

where  $p$  is a geometrical factor related to the interstitial vacancy network (1D, 2D, or 3D),  $\lambda$  is the hopping distance,  $\nu^*$  is the vibrational frequency, and  $E_B$  is the activation barrier for hopping, or the maximum energy point between the initial and final site of the diffusing ion. It is this activation barrier that will be affected by changes due to the interlayer environment, including the presence of interlayer molecules. As in the case of the activation energy barrier for charge transfer, the exponential dependence of the diffusion coefficient on  $E_B$  indicates that even small changes in the diffusion environment will lead to significant changes in the diffusion coefficient.

## V. INTERLAYER MODIFICATION OF LAYERED METAL OXIDES

Layered oxides form because of strong, directional bonding between oxygen and transition metal ions that results in the formation of weakly bonded atoms separated by large bonding distances. Therefore the general characteristic of layered structures is that there exists strong, covalent-ionic bonding within layers and weak, van der Waals bonding between layers. The interlayer binding energy for most layered compounds has been shown to be  $\sim 20 \text{ meV}/\text{\AA}^2$  by computational methods.<sup>55</sup> In comparison, the cleavage energy for a nonlayered compound such as NiO was calculated to be  $333 \text{ meV}/\text{\AA}^2$ ,<sup>56</sup> or approximately 16 times the energy of the interlayer bonding. In oxides, individual layers are negatively charged<sup>57</sup> so the interlayer may be modified by charged or polar species. The interaction between the interlayer species and the layers can be weak, so the species themselves can be fairly mobile and thus removed via



solvent exchange (the application of a concentration gradient) or, if they are charged, by application of an electric field. This section will highlight the means by which the interlayer spacing of layered oxides can be modified and the effect this has on the electrochemical energy storage properties.

### A. Structural water

Interlayer water molecules can be present within a layered structure by three different means: (i) as structural water present in the as-synthesized oxide; (ii) as a result of water diffusion into the interlayer spacing; and (iii) via electrochemical cycling in aqueous electrolytes. This section will focus on layered oxides with structural water, which include  $\text{WO}_3 \cdot n\text{H}_2\text{O}$ ,<sup>58</sup>  $\text{MoO}_3 \cdot n\text{H}_2\text{O}$ ,<sup>59</sup>  $\text{V}_2\text{O}_5 \cdot n\text{H}_2\text{O}$ ,<sup>60</sup> and birnessite ( $\delta$ )  $\text{MnO}_2$ .<sup>61</sup> In particular, the molybdenum and tungsten oxides form a series of stable and metastable hydrous phases. The stable phases include monoclinic  $\text{WO}_3 \cdot 2\text{H}_2\text{O}$ ,  $\text{WO}_3 \cdot \text{H}_2\text{O}$ ,  $\text{MoO}_3 \cdot 2\text{H}_2\text{O}$ , and  $\text{MoO}_3 \cdot \text{H}_2\text{O}$ . The dihydrates and monohydrates of tungsten and molybdenum are isostructural; the structures of the tungsten oxide hydrates are shown in Fig. 4. These hydrates are built up of corner-sharing and tilted octahedra. In the case of the monohydrate, the water is located at the apex of the octahedra whereas in the dihydrate, the second water is hydrogen bonded within the interlayer.

The effect of structural water on electrochemical energy storage has been investigated with molybdenum oxide hydrates cycled in nonaqueous lithium ion electrolytes. Nazri et al.<sup>62</sup> reported that molybdenum oxide hydrates ( $\text{MoO}_3 \cdot \text{H}_2\text{O}$  and  $\text{MoO}_3 \cdot 2/3\text{H}_2\text{O}$ ) exhibited higher capacity and better cyclability than anhydrous  $\text{MoO}_3$ . Kumagai et al.<sup>63</sup> reported that the  $\text{Li}^+$  intercalated into the structure in between the hydrated layers, and, in the monohydrate, obtained capacities of up to 400 mA h/g

at a current density of 0.2 mA/cm<sup>2</sup> between 3 and 1 V versus  $\text{Li/Li}^+$ . Due to the potential range for intercalation (3.5–1.5 V versus  $\text{Li/Li}^+$ ) and lack of Li in the as-synthesized structure, the materials are best suited as cathodes for primary batteries or anodes for hybrid electrochemical capacitors.

In aqueous electrolytes, interlayer water molecules have been hypothesized to provide rapid diffusion channels for protons. The Grotthius mechanism of proton diffusion<sup>51</sup> has been proposed in hydrated tunnel structures, such as those formed by hexagonal  $\text{MoO}_3$ , and is expected to occur in layered structures as well.<sup>64</sup> This mechanism accounts for the rapid diffusion of protons in aqueous electrolytes via the formation and deformation of hydrogen bonds on water molecules.<sup>65</sup> However, it is not clear whether the Grotthius mechanism occurs in all hydrated layered oxides. Recent density functional theory calculations indicated that protons do not intercalate via the water network in  $\text{WO}_3 \cdot 2\text{H}_2\text{O}$ ; instead, it was theorized that the mechanism of proton intercalation is binding to a bridging oxygen, the same as in  $\text{WO}_3$ .<sup>66</sup> On the other hand, experimental results of electrochromic hydrated tungsten oxides show rapid coloration and bleaching in acidic electrolytes, which was ascribed to rapid proton diffusion via the Grotthius mechanism.<sup>67</sup> The room temperature proton conductivity at ~50% relative humidity of  $\text{WO}_3 \cdot n\text{H}_2\text{O}$  was determined to be  $\sim 1 \times 10^{-5}$  S/cm for the dihydrate and monohydrate, and the proton conduction was hypothesized to occur via the interlayer hydrogen bonded network as in the Grotthius mechanism.<sup>68</sup> These diverse results underscore the need for in-depth understanding of transport mechanisms during electrochemical intercalation in hydrated structures.

In addition to the potential for rapid proton diffusion via the Grotthius mechanism, the presence of interlayer water molecules has been correlated with improved

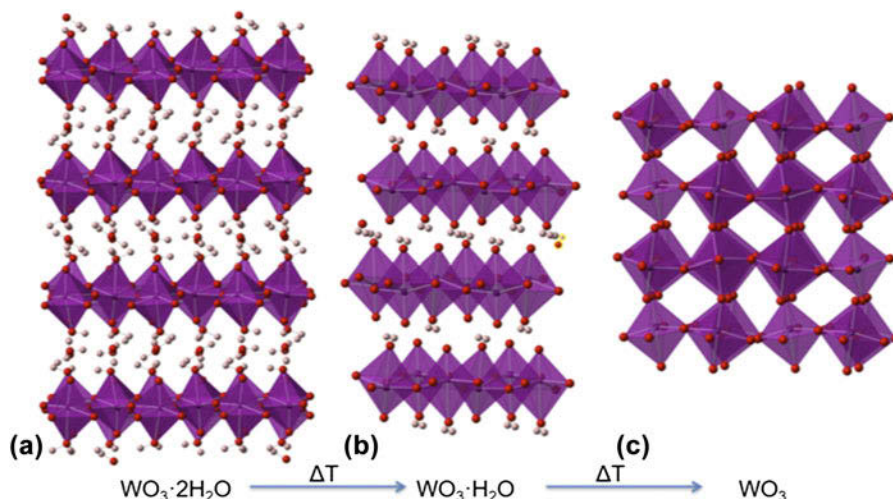


FIG. 4. Relationship between crystal structure and temperature of  $\text{WO}_3$  hydrates.  $\text{MoO}_3$  hydrates are isostructural with the tungsten oxide hydrates.

intercalation kinetics of multivalent ions. Multivalent ions are those with a formal charge greater than 1; of particular interest to energy storage applications is the storage of the divalent cation  $\text{Mg}^{2+}$ . This is because Mg metal, with a theoretical capacity of 2205 mA h/g (for the reaction  $\text{Mg}^{2+} + 2\text{e}^- \leftrightarrow \text{Mg}$ )<sup>69</sup> can be reversibly cycled in a suitable nonaqueous Mg-ion electrolyte without the formation of dendrites, as in the case of lithium metal. Thus the use of Mg metal as an anode allows for achieving both high energy density and safety. One of the challenges of Mg batteries, however, is finding a high voltage and high capacity cathode material. Intercalation of  $\text{Mg}^{2+}$  is not as facile as  $\text{Li}^+$  due to the sluggish solid state diffusion of  $\text{Mg}^{2+}$ , which is due to (i) the Coulombic repulsion between the framework transition metals and the diffusing  $\text{Mg}^{2+}$  ions, (ii) the need for a transition metal to accept  $2\text{e}^-$ , which results in an increase in the ionic radius and thus unit cell volume,<sup>70</sup> and (iii) the strong solvation<sup>71</sup> and anion coordination<sup>49</sup> of  $\text{Mg}^{2+}$ , which raises the activation energy for charge-transfer at the electrode/electrolyte interface.

The presence of interlayer water molecules can enable the reversible intercalation of  $\text{Mg}^{2+}$  because these species can act as a solvation shell, and shield the diffusing divalent cation from the lattice anions and cations.<sup>72</sup> For example,  $\text{V}_2\text{O}_5$  aerogels are high-surface area oxide materials made via supercritical drying of a  $\text{V}_2\text{O}_5$  gel.<sup>73,74</sup> Their short-range structure is similar to that of  $\text{V}_2\text{O}_5$  xerogels,<sup>75</sup> which consists of  $\text{V}_2\text{O}_5$  bilayers separated from each other by a large interlayer spacing ( $\sim 11.5$  Å) filled with water molecules. In the case of the aerogels, the nominal formula after supercritical drying is  $\text{V}_2\text{O}_5 \cdot 2\text{H}_2\text{O}$  and  $\sim 1.5$   $\text{H}_2\text{O}$  molecules are removed by heat treatment at  $120^\circ\text{C}$ .<sup>73</sup> The maximum amount of intercalation in the aerogel is  $\sim 0.6$   $\text{Mg}^{2+}$  per  $\text{V}_2\text{O}_5$ <sup>76,77</sup> which corresponds to a gravimetric capacity of 88 mA h/g. Figure 5(b) shows the cyclic voltammogram of a  $\text{V}_2\text{O}_5 \cdot 0.5\text{H}_2\text{O}$  aerogel in  $\text{Mg}(\text{ClO}_4)_2$  in propylene

carbonate electrolyte. It should be noted that while  $\text{Mg}^{2+}$  intercalation is reversible in  $\text{V}_2\text{O}_5$  aerogels, the separation between the cathodic ( $\text{Mg}^{2+}$  intercalation) and anodic ( $\text{Mg}^{2+}$  deintercalation) peaks is larger than in the case of  $\text{Li}^+$  intercalation [Fig. 5(a)], indicating that kinetics are still sluggish despite the benefit of interlayer water.

One potential drawback of structural water is that it may be removed during electrochemical cycling, leading to changes in the energy storage behavior, crystal structure, and potential contamination of a non-aqueous electrolyte with water.<sup>72</sup> The significance of this issue on the stability of interlayer structural water during electrochemical cycling varies. In the case of  $\text{V}_2\text{O}_5$  aerogels, Le et al.<sup>77</sup> used chemical analysis to determine that structural water was retained after chemical and electrochemical intercalation of  $\text{Li}^+$  and  $\text{Mg}^{2+}$ . On the other hand, Novák et al.<sup>78</sup> reported that structural water was removed upon repeated electrochemical intercalation and deintercalation of  $\text{Mg}^{2+}$  in hydrated layered vanadium oxide bronzes of the family  $\text{MV}_3\text{O}_8 \cdot n\text{H}_2\text{O}$ , where  $\text{M} = \text{Li}, \text{Na}, \text{K}, \text{Ca}_{0.5}, \text{and } \text{Mg}_{0.5}$ , and this group reported the same water loss in  $\text{V}_2\text{O}_5$  xerogel. The decrease in structural water content was correlated with decreased capacity for  $\text{Mg}^{2+}$  in the materials. Recently, the decrease in capacity of  $\text{V}_2\text{O}_5 \cdot 0.6\text{H}_2\text{O}$  with cycling in a  $\text{Li}^+$  nonaqueous electrolyte was correlated with accumulation of  $\text{LiOH}$ .<sup>79</sup> In the case of  $\text{MoO}_3 \cdot n\text{H}_2\text{O}$  cycled in a nonaqueous  $\text{Li}^+$  electrolyte, the decrease in capacity with cycling of anhydrous  $\text{MoO}_3$  was greater than that of the hydrous phases,  $\text{MoO}_3 \cdot \text{H}_2\text{O}$  and  $\text{MoO}_3 \cdot \frac{1}{3}\text{H}_2\text{O}$ .<sup>62</sup> Kumagai et al.<sup>63</sup> proposed that electrochemically intercalated  $\text{Li}^+$  react with the interlayer water molecules of  $\text{MoO}_3 \cdot 2\text{H}_2\text{O}$  because of the observed poor reversibility and decrease in interlayer spacing upon  $\text{Li}^+$  intercalation from *ex situ* XRD; the monohydrate was more stable. Based on these reports, it is possible that the removal and reactivity of interlayer water is more likely in structures where the water molecules are bound via hydrogen bonds to the interlayer, and not covalently bound as in the case of  $\text{MoO}_3 \cdot \text{H}_2\text{O}$ .

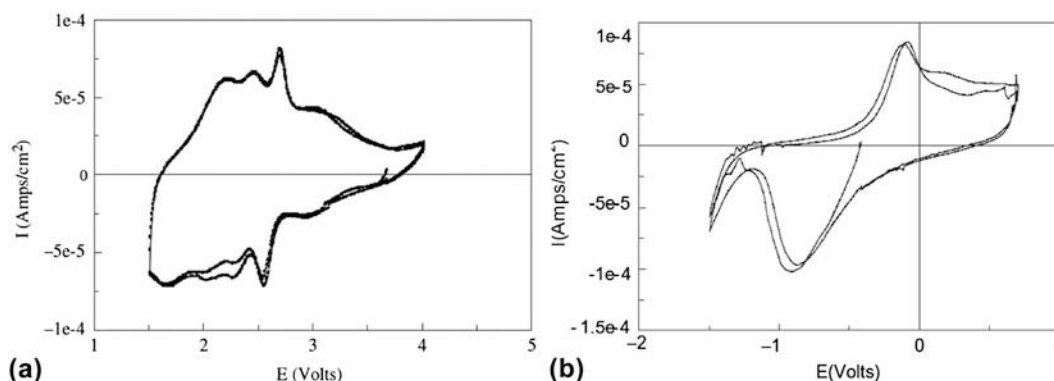
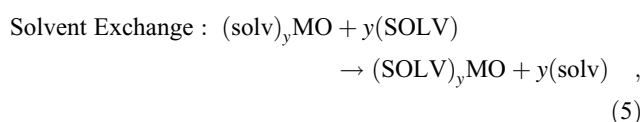
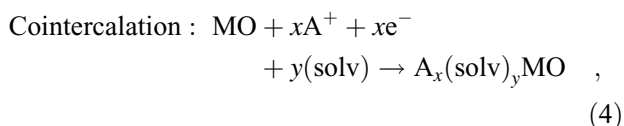


FIG. 5. Cyclic voltammetry of  $\text{V}_2\text{O}_5 \cdot 0.5\text{H}_2\text{O}$  aerogel in (a)  $\text{LiClO}_4$  in propylene carbonate and (b)  $\text{Mg}(\text{ClO}_4)_2$  in propylene carbonate electrolytes at  $0.1$  mV/s. The aerogel can be reversibly cycled in both electrolytes due to the nanostructured morphology and presence of structural water. Reprinted from Ref. 76, with permission from Elsevier.

## B. Solvent cointercalation & exchange

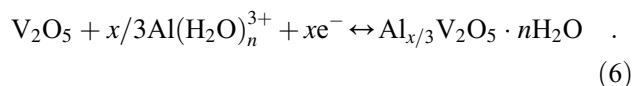
The previous section discussed the behavior of layered crystal structures with interlayer water molecules present in the as-synthesized state. For other layered structures, water and other polar solvent molecules may be intercalated during electrochemical cycling (so-called co-intercalation) or by solvent exchange.<sup>57</sup> Adapting the nomenclature established by Schöllhorn<sup>80</sup> these reactions can be written as:



where MO is a layered oxide,  $\text{A}^+$  is metal cation, and SOLV and solv represent two different solvents. These reactions present an additional mechanism for the control of the interlayer of transition metal oxides for electrochemical energy storage.

Solvent cointercalation has been investigated for improving the kinetics of  $\text{Mg}^{2+}$  energy storage. Using first-principles calculation, Gautam et al.<sup>81</sup> found that the cointercalation of water with  $\text{Mg}^{2+}$  into xerogel  $\text{V}_2\text{O}_5$  in nonaqueous electrolytes can increase the intercalation potential. Previously, Levi et al.<sup>72</sup> proposed that the increase in potential occurs because the intercalating ion does not need to shed a solvation shell (or does so only partially) during the charge-transfer step. Solvent cointercalation can be used to synthesize electrochemically active materials, such as the transformation of spinel  $\text{Mn}_3\text{O}_4$  into  $\delta\text{-MnO}_2$  in aqueous electrolytes.<sup>52,82</sup> Such hydrated  $\delta\text{-MnO}_2$  has been investigated as a potential cathode material for Mg ion batteries.<sup>52,82,83</sup> The improved intercalation kinetics and reversibility of  $\text{Mg}^{2+}$  in  $\delta\text{-MnO}_2$  have been ascribed to efficient Coulombic screening of the intercalating  $\text{Mg}^{2+}$  from the host structure by interlayer water molecules [Fig. 6(a)]. First, spinel  $\text{Mn}_3\text{O}_4$  was cycled in an aqueous  $\text{Mg}^{2+}$  electrolyte to form hydrated, layered  $\delta\text{-MnO}_2$ . Then, the material was cycled in a nonaqueous  $\text{Mg}^{2+}$  electrolyte with varying amounts of water. Compared with the completely anhydrous electrolyte, hydrated  $\delta\text{-MnO}_2$  cycled in a  $\text{Mg}^{2+}$  nonaqueous electrolyte with small amounts of water showed higher capacity and lifetime [Figs. 6(b) and 6(c)]. However, Sun, et al. found that the hydrated material undergoes a conversion reaction with  $\text{Mg}^{2+}$  in a nonaqueous electrolyte with the formation of  $\text{MnOOH}$ ,  $\text{MnO}$ , and  $\text{Mg}(\text{OH})_2$ ; reversible intercalation was only observed in an aqueous  $\text{Mg}^{2+}$  electrolyte.<sup>83</sup>

The benefits of water co-intercalation for the reversibility of multivalent ion intercalation are not limited to  $\text{Mg}^{2+}$ . González et al.<sup>84</sup> reported on the reversible charge storage of  $\text{Al}^{3+}$  from an aqueous electrolyte into  $\text{V}_2\text{O}_5$  xerogel and proposed a co-intercalation reaction mechanism:



Since  $\text{Al}^{3+}$  is a small cation (ionic radius of 0.68 Å) with a large charge, it has a high standard hydration enthalpy, which means that it is very strongly hydrated. Therefore, it is reasonable to assume that solid state intercalation of  $\text{Al}^{3+}$  can only occur via solvent cointercalation, otherwise, the activation energy for charge transfer at the interface is too high.

Solvent exchange of water for other polar molecules can be performed in structures that contain water in the as-synthesized state or in anhydrous layered oxides whose interlayer bonding is weak enough that solvent molecules may intercalate. Molybdenum oxides serve as model systems for investigating solvent exchange because both hydrated and anhydrous crystalline  $\text{MoO}_3$  form layered structures,<sup>85</sup> which expands the number of precursors that can be used for solvent exchanged  $\text{MoO}_3$ . Schöllhorn et al.<sup>57</sup> performed solvent exchange of  $\text{Na}_{0.5}(\text{H}_2\text{O})_y\text{MoO}_3$  bronze with dimethylsulfoxide (DMSO); the interlayer spacing increased from 11.41 to 16.92 Å. In a related experiment,  $\text{Na}_{0.5}(\text{H}_2\text{O})_y\text{MoO}_3$  bronze was used to intercalate various organic compounds; interlayer spacings as large as 37.9 Å were reported for  $\text{MoO}_3$  intercalated with tetradecylamine.<sup>86</sup> Chen et al.<sup>87</sup> utilized  $\text{MoO}_3 \cdot \text{H}_2\text{O}$  as the precursor for the solvent exchange of water with *n*-octylamines in ethanol. The reaction was described as an acid–base reaction between the water molecules and amines. The amines occupy the interlayer space in a bilayer arrangement with a 51° tilt angle and with an expanded interlayer spacing of 23.1 Å, as illustrated in Fig. 7; heat treatment of the materials at 550 °C yields anhydrous  $\text{MoO}_3$ . The electrochemistry of these materials was not reported and bears further investigation as such large interlayer spacings may be beneficial for multivalent and high-rate intercalation.

## C. Cation exchange

Layered metal oxides may also undergo cation exchange. In transition metal oxides, the layers are negatively charged and can thus accommodate cationic interstitial guest species. For cation exchange, the starting material may contain the exchangeable ion in the as-synthesized state (e.g.,  $\text{LiCoO}_2$ ) or as a result of electrochemical cycling (e.g.,  $\text{Li}_x\text{V}_2\text{O}_5$ ). Cation exchange may occur by the exchange of only the

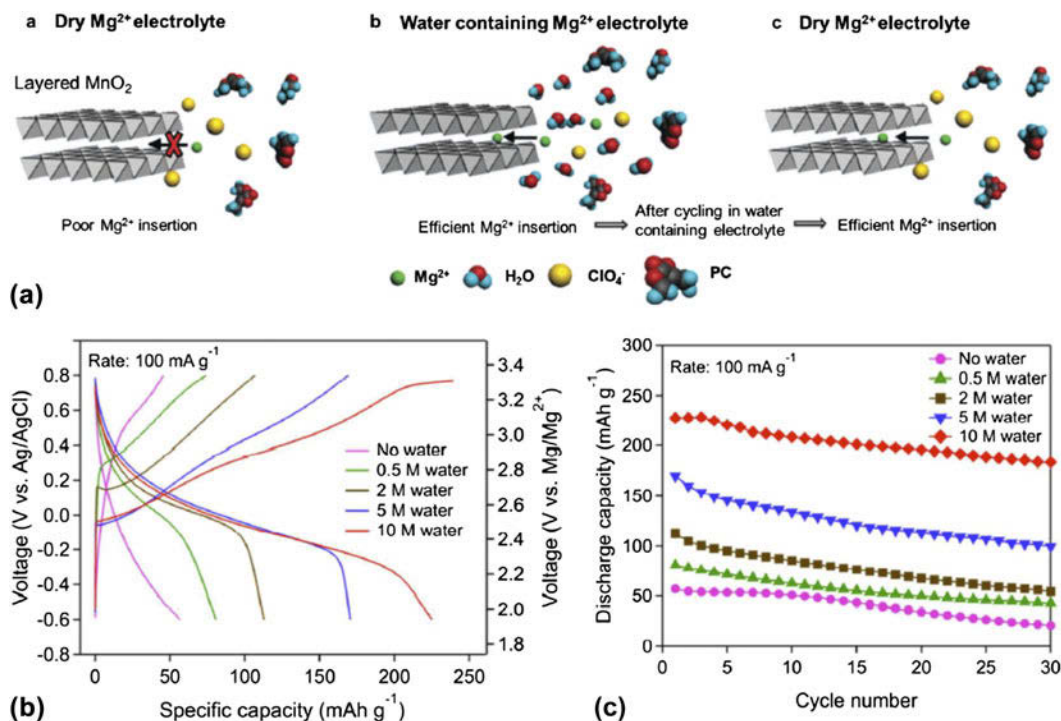


FIG. 6. (a) Proposed mechanism for the enhanced electrochemical energy storage of  $\text{Mg}^{2+}$  in layered  $\delta\text{-MnO}_2$ . Reproduced from Ref. 82 with permission of the PCCP Owner Societies. (b) Galvanostatic charge/discharge of  $\delta\text{-MnO}_2$  in  $\text{Mg}^{2+}$  non-aqueous electrolyte with different water content, and (c) capacity versus cycle number of the same system. Reprinted with permission from Ref. 52. Copyright 2015 American Chemical Society.

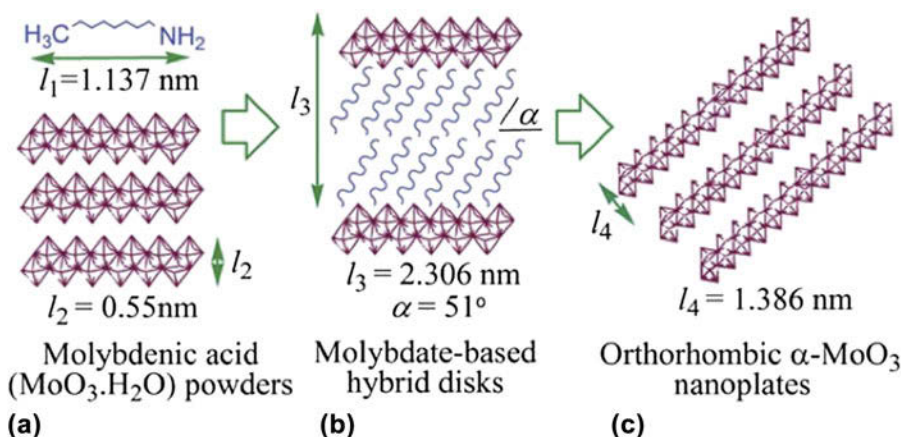


FIG. 7. Synthesis of a  $\text{MoO}_3$ -alkylamine hybrid starting from (a)  $\text{MoO}_3 \cdot \text{H}_2\text{O}$  precursor, (b) structure of the inorganic-organic hybrid including orientation of alkyl amine chains, (c) thermal heat treatment at  $550^\circ\text{C}$  yields orthorhombic  $\alpha\text{-MoO}_3$ . Reproduced from Ref. 87 with permission of The Royal Society of Chemistry.

cation or with solvent co-intercalation, as described above. A recent review summarized the general features of cation exchange in nanoscale materials.<sup>88</sup>

The desire to improve the electrochemical behavior of lithium ion cathode materials has focused significant effort on the cation exchange of layered metal oxides.  $\text{LiCoO}_2$  is a prototypical Li-ion battery cathode material whose structure consists of alternating layers of lithium and cobalt separated by oxygen layers in an ...ABCABC...

stacking sequence.<sup>89</sup> A low-temperature route for the synthesis of  $\text{LiCoO}_2$  and  $\text{LiNiO}_2$  was proposed by Larcher et al.<sup>90</sup> who performed the cation exchange of  $\text{NiOOH}$  and  $\text{CoOOH}$  in a hydrothermal reactor in the presence of  $\text{LiOH}$ ; Fig. 8 shows the topotactic nature of the cation exchange. The oxyhydroxides are similar in structure to the  $\text{LiMO}_2$  ( $\text{M} = \text{Ni}, \text{Co}$ ). In the case of  $\text{LiCoO}_2$ , the electrochemical behavior of the cation-exchanged phase was inferior to the high temperature



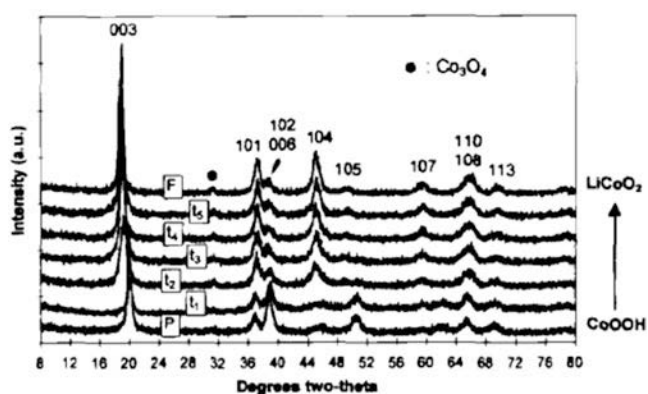


FIG. 8. XRD patterns as a function of the extent of cation exchange of CoOOH ( $\text{HCoO}_2$ ) to  $\text{LiCoO}_2$ . Reprinted with permission from Ref. 90. Copyright 1997, The Electrochemical Society.

phase due to lower coulombic efficiency. On the other hand, cation exchanged  $\text{LiNiO}_2$  exhibited similar capacity and reversibility as the high temperature analog. The increased surface area of the cation exchanged  $\text{LiNiO}_2$  did result in increased moisture sensitivity as compared to the high temperature phase,<sup>90</sup> thus exacerbating the well-known surface instability issues of  $\text{LiNiO}_2$ .<sup>91</sup>

Cation exchange is also useful as a low temperature method to synthesize metastable phases. A well-known example is the cation exchange synthesis of  $\text{LiMnO}_2$ , reported by Armstrong et al.<sup>92</sup> and Capitaine et al.<sup>93</sup> by stirring  $\text{NaMnO}_2$  in  $\text{LiCl}$  or  $\text{LiBr}$  in alcohol. However, during electrochemical cycling, the obtained  $\text{LiMnO}_2$  with an  $\text{O}_3$  layered structure undergoes conversion to a more stable spinel phase.<sup>94</sup> Therefore, one of the challenges of synthesis via cation exchange is that the structure may convert to a more stable phase during prolonged electrochemical cycling.

#### D. Polymers and small molecules

Some structures can exhibit very large interlayer spacings that can accommodate not just solvent molecules or cations, but polymers. Of interest for electrochemical energy storage are compounds that will increase the capacity by providing additional redox active sites or that will increase the electronic conductivity of the oxide to increase the rate capability. An example of a polymer that can provide both is polyaniline (PANI), which can be intercalated into  $\text{V}_2\text{O}_5$  xerogels, with a resulting interlayer spacing of 14–19 Å.<sup>95</sup> As shown in Fig. 9(a), the PANI is only present within the interlayer. Figure 9(b) shows the galvanostatic charge/discharge of nanostructured  $\text{V}_2\text{O}_5$  and  $\text{V}_2\text{O}_5/\text{PANI}$  nanocomposite; the capacity of the polymer-intercalated oxide was approximately doubled at the same time that the electronic conductivity increased  $\sim 50$  times.<sup>96</sup>

#### E. Exfoliation

An important property of bulk layered oxides is that they can be completely exfoliated into mono- or few-layer sheets (‘nanosheets’). There has been significant interest in discovering the electrochemical energy storage properties of such materials because, in theory, they exhibit short diffusion distances and a large number of surface redox sites<sup>98,99</sup> which could lead to high power and high energy density storage. In this regard, the methods of modifying the interlayer described above have all been utilized as a means to expand the interlayer spacing of layered oxides, which decreases the force needed to pull apart the layers into nanosheets. The applied force can be mechanical,<sup>100</sup> acoustic,<sup>101</sup> thermal,<sup>102</sup> or a combination of these.<sup>103</sup> Figure 10 shows the general mechanism of exfoliation of layered materials into few-layer sheets.<sup>18</sup> A recent review described synthesis methods for controlling nanosheet size, composition, and structure.<sup>104</sup>

Such exfoliated layered oxide nanosheets have primarily been investigated for use as electrochemical capacitor electrodes, and specifically as pseudocapacitors.<sup>25</sup> This is because the nanosheet architecture would ideally expose all of the redox active sites directly to the electrolyte and enable rapid charge-transfer reactions with minimal solid state diffusion. As noted previously,  $\text{MoO}_3$  forms both hydrous and anhydrous layered polymorphs and it is a good precursor material for the synthesis of nanosheets. Bulk crystalline  $\text{MoO}_3$  can be exfoliated by sonicating a dispersion of the oxide in a solution of water and isopropanol<sup>101</sup>; the mechanism of exfoliation is the intercalation of isopropanol between  $\text{MoO}_3$  layers and subsequent application of acoustic energy in the form of sonication. Hanlon et al.<sup>105</sup> synthesized  $\text{MoO}_3$  nanosheets via liquid-phase exfoliation that consisted of sonicating  $\text{MoO}_3$  in isopropanol. Figure 11 shows the dispersion, absorbance, and TEM of the exfoliated nanosheets separated by size into small, very small, and large; the size selection was obtained by centrifuging the stock solution at different speeds and selecting the supernatant. The maximum capacitance ( $\sim 200 \text{ F/g}^1$  at 10 mV/s or 200 s) was obtained by combining the exfoliated  $\text{MoO}_3$  nanosheets with carbon nanotubes.

The benefits of synthesizing nanosheets from exfoliated bulk oxides is that this technique is readily scalable.<sup>18</sup> However, there are several challenges for using exfoliated nanosheets as energy storage materials for large-scale devices.<sup>44</sup> The high surface area of nanosheets can lead to increased side reactions with the electrolyte, which have to be avoided for long cycle life and safety. Second, the high surface area can also lead to low volumetric capacity/capacitance as compared with the bulk materials. Third, such materials contain many defects that can lead to limited cycle life and barriers

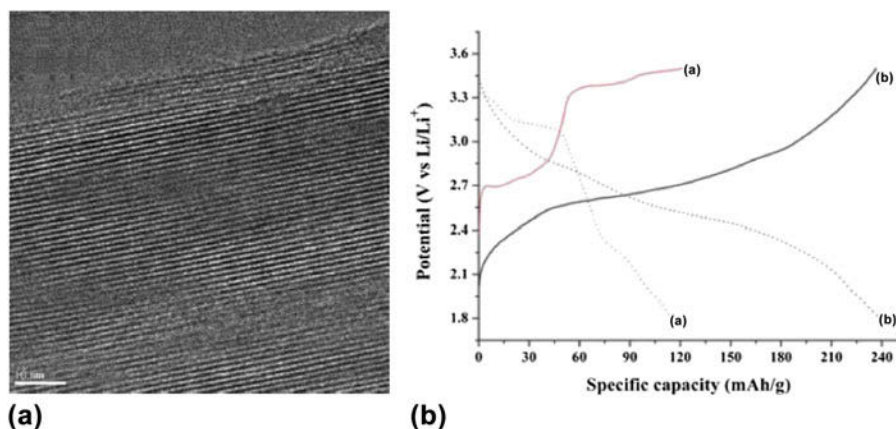


FIG. 9. (a) TEM of a vanadium oxide/polyaniline composite, where the polyaniline is inserted into the interlayer spacing of the oxide. Reprinted from Ref. 97, with permission from Elsevier. (b) Galvanostatic charge/discharge of nanostructured  $V_2O_5$  (curve “a”) and  $V_2O_5$ /PANI nanocomposite (curve “b”) in a non-aqueous  $Li^+$  electrolyte at a current density of 29.5 mA/g. Reproduced from Ref. 96 with permission of The Royal Society of Chemistry.

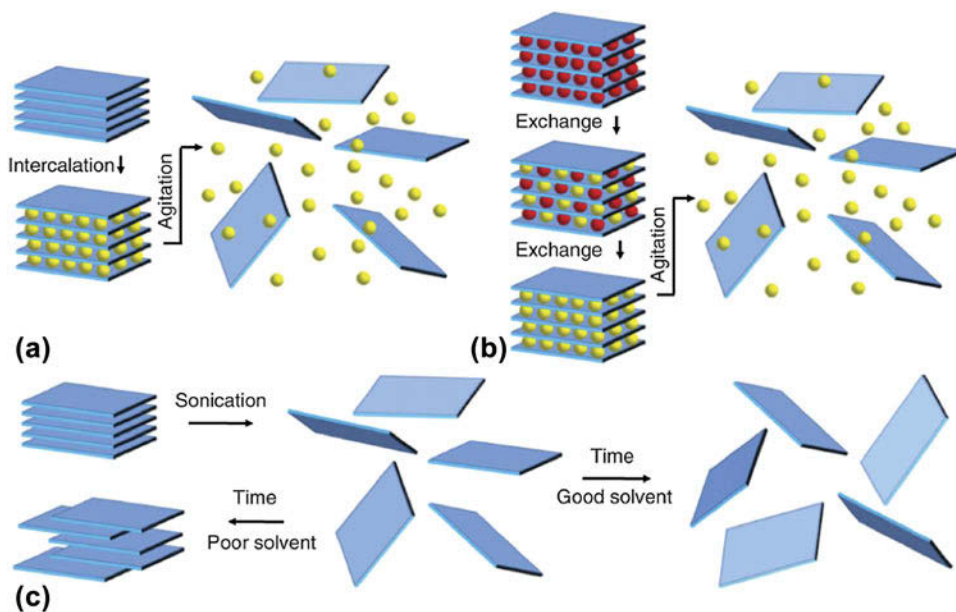


FIG. 10. Schematic description of exfoliation mechanisms of layered materials to yield nanosheets: (a) intercalation followed by agitation; (b) ion exchange followed by agitation; (c) direct agitation via sonication. From Ref. 18. Reprinted with permission from AAAS.

for ion diffusion. On the other hand, nanosheets can be highly advantageous for small-scale energy storage devices.<sup>106</sup> Also, restacked exfoliated nanosheets have recently been reported as precursors for the synthesis of Li-ion battery cathode materials, presenting an interesting strategy for the development of metastable layered oxides.<sup>107</sup>

## F. Exfoliated metal oxide heterostructures

Exfoliated layered oxide materials can be assembled into new heterostructured layered oxide materials.<sup>108</sup> The motivation for synthesizing such materials is that they can exhibit improved properties over the individual

components. In the case of oxide materials, this typically means improving their electronic conductivity to enable higher rate capability by forming heterostructures with graphene. One example of this method is the synthesis of graphene/ $MnO_2$  hybrids via co-exfoliation for use as electrochemical capacitors.<sup>109</sup> The highest capacitance was obtained with the co-exfoliated materials (as opposed to the individual components); a volumetric capacitance of 200 F/cm<sup>3</sup> was obtained at a sweep rate of 100 mV/s (charge/discharge time of 10 s). The synthesis of these heterostructures opens up the possibility of entirely new metal oxide/hybrid materials assembled at the atomic layer. Most of these composites; however, are synthesized via self-assembly<sup>110,111</sup> as opposed to bulk exfoliation.

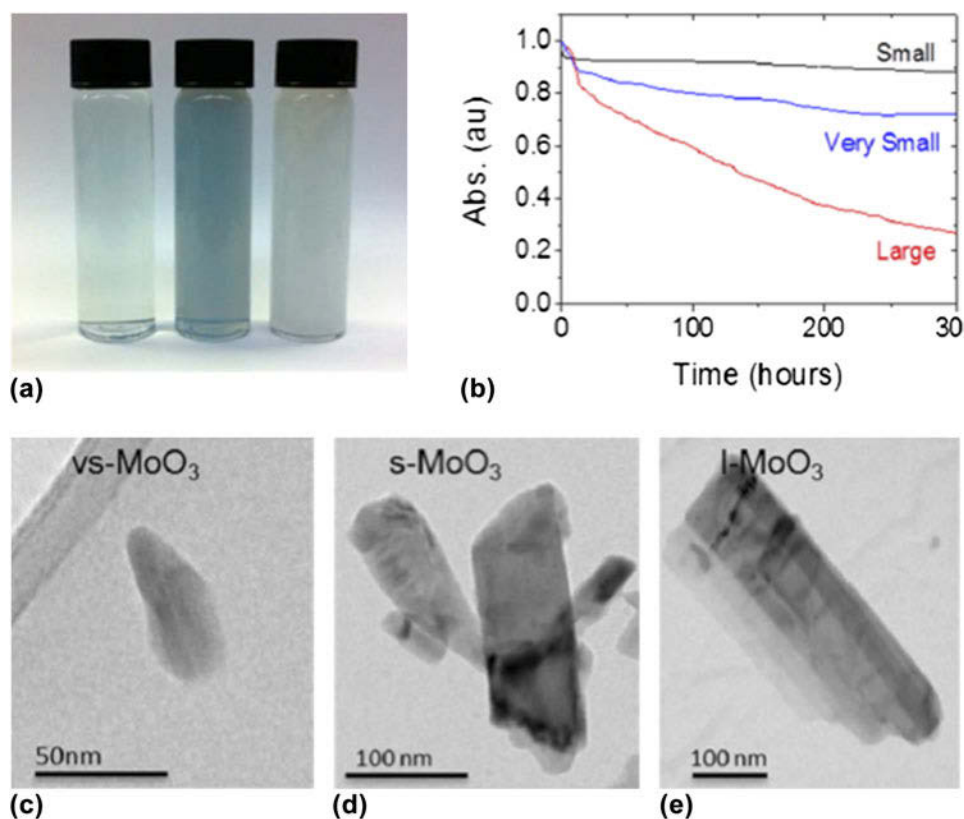


FIG. 11. Synthesis of MoO<sub>3</sub> nanosheets via liquid exfoliation of bulk MoO<sub>3</sub>: (a) dispersions of (left to right) very small, small, and large nanosheets; (b) measurement of sedimentation via absorption as a function of time; (c) TEM of very small MoO<sub>3</sub> nanosheets; (d) small MoO<sub>3</sub> nanosheets; and (e) large MoO<sub>3</sub> nanosheets.<sup>105</sup> Reprinted with permission from Ref. 105. Copyright 2014 American Chemical Society.

## VI. FUTURE OUTLOOK & CONCLUSIONS

Layered oxides have played a key role in the development of high energy density electrochemical storage, from the investigations of alkali ion intercalation in oxides in the 1970s by Whittingham<sup>112</sup> to the identification of LiCoO<sub>2</sub> cathodes by Goodenough<sup>113</sup> in the early 1980 to subsequent commercialization of high energy density lithium-ion batteries for portable electronics. In the future, layered oxides will continue to be utilized as electrodes in next generation devices including advanced lithium-ion batteries, sodium-ion batteries, and electrochemical capacitors, that take advantage of their energy density, power density, environmental stability, high potential, and lifetime. Within this class of materials, the vacant site for energy storage can be modified, and this presents a unique ‘control knob’ to tune the atomic and nanoscale electrochemical environment of bulk oxides that is not readily available in other structures.

The interlayer can be modified by the presence of structural or co-intercalated water and solvent molecules, cation exchange, or polymeric and molecules species. These can enhance the charge transfer by increasing the interlayer spacing to allow solvent co-intercalation, or for partial solvation of the intercalating ion within the

interlayer. Diffusion in the bulk can be enhanced by allowing either fast transport (e.g., proton hopping via hydrogen bonding) or, in the case of multivalent ion intercalation, partial charge screening. Further research is needed to understand the exact mechanisms and lifetime of interlayer modified materials and to extend these methods from model layered oxides such as V<sub>2</sub>O<sub>5</sub> and MoO<sub>3</sub> to cathode materials such as LiCoO<sub>2</sub>. There has been some recent promising work in this area for non-aqueous sodium-ion batteries. For example, interlayer modification of layered sodium metal oxide cathodes by doping of the interlayer with small amounts of Li<sup>114</sup> or Mg<sup>115</sup> improves the cycling stability by stabilizing the structure. The continuing need for better electrochemical energy storage, coupled with improvements in characterization capability and synthesis techniques, will push the properties of layered metal oxides forward. The methods of interlayer modification are an important design tool in the development of these advanced materials.

## ACKNOWLEDGMENT

The author acknowledges start up funding from North Carolina State University.

## REFERENCES

1. Nasa Global Climate change Vital Signs: CO<sub>2</sub>. <http://climate.nasa.gov/vital-signs/carbon-dioxide/> (accessed August 13, 2016).
2. X.H. Liu and J.Y. Huang: In situ TEM electrochemistry of anode materials in lithium ion batteries. *Energy Environ. Sci.* **4**(10), 3844 (2011).
3. Z. Wang, D. Santhanagopalan, W. Zhang, F. Wang, H.L. Xin, K. He, J. Li, N.J. Dudney, and Y.S. Meng: In situ STEM/EELS observation of nanoscale interfacial phenomena in all-solid-state batteries. *Nano Lett.* **16**, 3760 (2016).
4. C-M. Wang, W. Xu, J. Liu, J-G. Zhang, L.V. Saraf, B.W. Arey, D. Choi, Z-G. Yang, J. Xiao, S. Thevuthasan, and D.R. Baer: In situ transmission electron microscopy observation of microstructure and phase evolution in a SnO<sub>2</sub> nanowire during lithium intercalation. *Nano Lett.* **11**(5), 1874 (2011).
5. R. Kodama, Y. Terada, I. Nakai, S. Komaba, and N. Kumagai: Electrochemical and in situ XAFS–XRD investigation of Nb<sub>2</sub>O<sub>5</sub> for rechargeable lithium batteries. *J. Electrochem. Soc.* **153**(3), A583 (2006).
6. K-W. Nam, W-S. Yoon, H. Shin, K.Y. Chung, S. Choi, and X-Q. Yang: In situ x-ray diffraction studies of mixed LiMn<sub>2</sub>O<sub>4</sub>–LiNi<sub>1/3</sub>Co<sub>1/3</sub>Mn<sub>1/3</sub>O<sub>2</sub> composite cathode in Li-ion cells during charge–discharge cycling. *J. Power Sources* **192**(2), 652 (2009).
7. N. Sharma, W.K. Pang, Z. Guo, and V.K. Peterson: In situ powder diffraction studies of electrode materials in rechargeable batteries. *ChemSusChem* **8**(17), 2826 (2015).
8. A.N. Mansour, P.H. Smith, W.M. Baker, M. Balasubramanian, and J. McBreen: In situ XAS investigation of the oxidation state and local structure of vanadium in discharged and charged V<sub>2</sub>O<sub>5</sub> aerogel cathodes. *Electrochim. Acta* **47**(19), 3151 (2002).
9. M-K. Song, S. Cheng, H. Chen, W. Qin, K-W. Nam, S. Xu, X-Q. Yang, A. Bongiorno, J. Lee, J. Bai, T.A. Tyson, J. Cho, and M. Liu: Anomalous pseudocapacitive behavior of a nanostructured, mixed-valent manganese oxide film for electrical energy storage. *Nano Lett.* **12**(7), 3483 (2012).
10. J.P. Bearinger, C.A. Orme, and J.L. Gilbert: Direct observation of hydration of TiO<sub>2</sub> on Ti using electrochemical AFM: Freely corroding versus potentiostatically held. *Surf. Sci.* **491**(3), 370 (2001).
11. Y.S. Cohen and D. Aurbach: Surface films phenomena on vanadium-pentoxide cathodes for Li and Li-ion batteries: In situ AFM imaging. *Electrochem. Commun.* **6**, 536 (2004).
12. J.W. Bullard and R.L. Smith: Structural evolution of the MoO<sub>3</sub>(010) surface during lithium intercalation. *Solid State Ionics* **160**(3–4), 335 (2003).
13. J. Lei, F. McLarnon, and R. Kostecki: In situ Raman microscopy of individual LiNi<sub>0.8</sub>Co<sub>0.15</sub>Al<sub>0.05</sub>O<sub>2</sub> particles in a Li-ion battery composite cathode. *J. Phys. Chem. B* **109**, 952 (2005).
14. F. Texier, L. Servant, J.L. Bruneel, and F. Argoul: In situ probing of interfacial processes in the electrodeposition of copper by confocal Raman microspectroscopy. *J. Electroanal. Chem.* **446**(1–2), 189 (1998).
15. M. Meller, J. Menzel, K. Fic, D. Gastol, and E. Frackowiak: Electrochemical capacitors as attractive power sources. *Solid State Ionics* **265**, 61 (2014).
16. B. Wu, C. Guo, N. Zheng, Z. Xie, and G.D. Stucky: Nonaqueous production of nanostructured anatase with high-energy facets. *J. Am. Chem. Soc.* **130**, 17563 (2008).
17. I.E. Rauda, V. Augustyn, B. Dunn, and S.H. Tolbert: Enhancing pseudocapacitive charge storage in polymer templated mesoporous materials. *Acc. Chem. Res.* **46**(5), 1113 (2013).
18. V. Nicolosi, M. Chhowalla, M.G. Kanatzidis, M.S. Strano, and J.N. Coleman: Liquid exfoliation of layered materials. *Science* **340**(6139), 1226419 (2013).
19. D. Pech, M. Brunet, H. Durou, P. Huang, V. Mochalin, Y. Gogotsi, P-L. Taberna, and P. Simon: Ultrahigh-power micrometre-sized supercapacitors based on onion-like carbon. *Nat. Nanotechnol.* **5**, 651 (2010).
20. S.K. Cheah, E. Perre, M. Rooth, M. Fondell, A. Hårsta, L. Nyholm, M. Boman, J. Lu, P. Simon, and K. Edstro: Self-supported three-dimensional nanoelectrodes for microbattery applications. *Nano Lett.* **9**, 3230 (2009).
21. J. Liu, J.G. Zhang, Z. Yang, J.P. Lemmon, C. Imhoff, G.L. Graff, L. Li, J. Hu, C. Wang, J. Xiao, G. Xia, V.V. Viswanathan, S. Baskaran, V. Sprenkle, X. Li, Y. Shao, and B. Schwenzer: Materials science and materials chemistry for large scale electrochemical energy storage: From transportation to electrical grid. *Adv. Funct. Mater.* **23**(8), 929 (2013).
22. R.M. Penner and Y. Gogotsi: The rising and receding fortunes of electrochemists. *ACS Nano* **10**(4), 3875 (2016).
23. A. Manthiram, A. Vadivel Murugan, A. Sarkar, and T. Muraliganth: Nanostructured electrode materials for electrochemical energy storage and conversion. *Energy Environ. Sci.* **1**(6), 621 (2008).
24. D. Kundu, E. Talaie, V. Duffort, and L.F. Nazar: The emerging chemistry of sodium ion batteries for electrochemical energy storage. *Angew. Chem., Int. Ed.* **54**(11), 3432 (2015).
25. V. Augustyn, P. Simon, and B. Dunn: Pseudocapacitive oxide materials for high-rate electrochemical energy storage. *Energy Environ. Sci.* **7**, 1597 (2014).
26. B.C. Bunker and W.H. Casey: *The Aqueous Chemistry of Oxides* (Oxford University Press, New York, 2016).
27. C.S. Johnson, N. Li, C. Lefief, J.T. Vaughey, and M.M. Thackeray: Synthesis, characterization and electrochemistry of lithium battery electrodes:  $x\text{Li}_2\text{MnO}_3 \cdot (1-x)\text{LiMn}_{0.333}\text{Ni}_{0.333}\text{Co}_{0.333}\text{O}_2$  ( $0 \leq x \leq 0.7$ ). *Chem. Mater.* **20**(19), 6095 (2008).
28. Y. Li, D. Wang, Q. An, B. Ren, Y. Rong, and Y. Yao: Flexible electrode for long-life rechargeable sodium-ion batteries: Effect of oxygen vacancy in MoO<sub>3-x</sub>. *J. Mater. Chem. A* **4**(15), 5402 (2016).
29. B.E. Conway: Electrochemical science and technology. Transition from “supercapacitor” to “battery” behavior in electrochemical energy storage. *J. Electrochem. Soc.* **138**(6), 1539 (1991).
30. M. Whittingham: Insertion electrodes as SMART materials: The first 25 years and future promises. *Solid State Ionics* **134**, 169 (2000).
31. R. Benedek, J. Vaughey, and M.M. Thackeray: Theory of overlithiation reaction in LiMO<sub>2</sub> battery electrodes. *Chem. Mater.* **18**(5), 1296 (2006).
32. P. Poizat, S. Laruelle, S. Grugeon, L. Dupont, and J-M.M. Tarascon: Nano-sized transition-metal oxides as negative-electrode materials for lithium-ion batteries. *Nature* **407**(6803), 496 (2000).
33. B.E. Conway and W.G. Pell: Double-layer and pseudocapacitance types of electrochemical capacitors and their applications to the development of hybrid devices. *J. Solid State Electrochem.* **7**(9), 637 (2003).
34. P. Simon and Y. Gogotsi: Capacitive energy storage in nanostructured carbon-electrolyte systems. *Acc. Chem. Res.* **46**, 1094 (2013).
35. B.E. Conway: *Electrochemical Supercapacitors: Scientific Fundamentals, and Technological Applications* (Kluwer-Academic, New York, 1999).
36. J.P. Zheng, P.J. Cygan, and T.R. Jow: Hydrous ruthenium oxide as an electrode material for electrochemical capacitors. *J. Electrochem. Soc.* **142**(8), 2699 (1995).
37. J. Wang, J. Polleux, J. Lim, and B. Dunn: Pseudocapacitive contributions to electrochemical energy storage in TiO<sub>2</sub> (anatase) nanoparticles. *J. Phys. Chem. C* **111**(40), 14925 (2007).



38. V. Augustyn, J. Come, M.A. Lowe, J.W. Kim, P-L. Taberna, S.H. Tolbert, H.D. Abruña, P. Simon, and B. Dunn: High-rate electrochemical energy storage through  $\text{Li}^+$  intercalation pseudocapacitance. *Nat. Mater.* **12**(6), 518 (2013).
39. N.A. Chernova, M. Roppolo, A.C. Dillon, and M.S. Whittingham: Layered vanadium and molybdenum oxides: Batteries and electrochromics. *J. Mater. Chem.* **19**(17), 2526 (2009).
40. J. Tarascon, S. Grugeron, M. Morcrette, S. Laruelle, P. Rozier, and P. Poizot: New concepts for the search of better electrode materials for rechargeable lithium batteries. *C. R. Chim.* **8**(1), 9 (2005).
41. C. Ban, Z. Wu, D.T. Gillaspie, L. Chen, Y. Yan, J.L. Blackburn, and A.C. Dillon: Nanostructured  $\text{Fe}_3\text{O}_4/\text{SWNT}$  electrode: Binder-free and high-rate Li-ion anode. *Adv. Mater.* **22**(20), E145 (2010).
42. J. Cabana, L. Monconduit, D. Larcher, and M.R. Palacín: Beyond intercalation-based Li-ion batteries: The state of the art and challenges of electrode materials reacting through conversion reactions. *Adv. Mater.* **22**(35), E170 (2010).
43. P. Poizot, S. Laruelle, S. Grugeron, and J-M. Tarascon: Rationalization of the low-potential reactivity of 3d-metal-based inorganic compounds toward Li. *J. Electrochem. Soc.* **149**(9), A1212 (2002).
44. M.R. Palacín, P. Simon, and J.M. Tarascon: Nanomaterials for electrochemical energy storage: The good and the bad. *Acta Chim. Slov.* **63**, 417–423 (2016).
45. F. Cheng, J. Liang, Z. Tao, and J. Chen: Functional materials for rechargeable batteries. *Adv. Mater.* **23**(15), 1695 (2011).
46. P.G. Bruce and M.Y. Saidi: The mechanism of electrointercalation. *J. Electroanal. Chem.* **322**(1–2), 93 (1992).
47. T. Okumura, T. Fukutsuka, K. Matsumoto, Y. Orikasa, H. Arai, Z. Ogumi, and Y. Uchimoto: Lithium-ion transfer reaction at the interface between partially fluorinated insertion electrodes and electrolyte solutions. *J. Phys. Chem. C* **115**(26), 12990 (2011).
48. K. Xu: “Charge-transfer” process at graphite/electrolyte interface and the solvation sheath structure of  $\text{Li}^+$  in nonaqueous electrolytes. *J. Electrochem. Soc.* **154**(4), A162 (2007).
49. L.F. Wan, B.R. Perdue, C.A. Apple, and D. Prendergast: Mg desolvation and intercalation mechanism at the  $\text{Mo}_6\text{S}_8$  Chevrel phase surface. *Chem. Mater.* **27**, 5932 (2015).
50. M. Park, X. Zhang, M. Chung, G.B. Less, and A.M. Sastry: A review of conduction phenomena in Li-ion batteries. *J. Power Sources* **195**(24), 7904 (2010).
51. M. Whittingham: Hydrogen motion in oxides: From insulators to bronzes. *Solid State Ionics* **168**(3–4), 255 (2004).
52. K.W. Nam, S. Kim, S-S. Lee, M. Salama, I. Shterenberg, Y. Gofer, J-S. Kim, E. Yang, C-S. Park, J-S. Kim, S-S. Lee, W-S. Chang, S.G. Doo, Y.N. Jo, Y. Jung, D. Aurbach, and J.W. Choi: The high performance of crystal water containing manganese birnessite cathodes for magnesium batteries. *Nano Lett.* **15**, 4071 (2015).
53. J. Song, E. Gillette, S.B. Lee, M. Noked, G.W. Rubloff, E. Gillette, J. Duay, G.W. Rubloff, and S.B. Lee: Activation of  $\text{MnO}_2$  cathode by water-stimulated  $\text{Mg}^{2+}$  insertion for magnesium ion battery. *Phys. Chem. Chem. Phys.* **17**(7), 5256 (2015).
54. A. Van der Ven, J. Bhattacharya, and A.A. Belak: Understanding Li diffusion in Li-intercalation compounds. *Acc. Chem. Res.* **46**, 1216 (2012).
55. T. Bjorkman, A. Gulans, A.V. Krashenninnikov, and R.M. Nieminen: Van der Waals bonding in layered compounds from advanced density-functional first-principles calculations. *Phys. Rev. Lett.* **108**(23), 1 (2012).
56. A. Wander, I. Bush, and N. Harrison: Stability of rocksalt polar surfaces: An ab initio study of  $\text{MgO}(111)$  and  $\text{NiO}(111)$ . *Phys. Rev. B* **68**(23), 1 (2003).
57. R. Schöllhorn, R. Kuhlmann, and J.O. Besenhard: Topotactic redox reactions and ion exchange of layered  $\text{MoO}_3$  bronzes. *Mater. Res. Bull.* **11**(1), 83 (1976).
58. M.L. Freedman: The tungstic acids. *J. Am. Chem. Soc.* **81**(15), 3834 (1959).
59. A. Kuzmin and J. Purans: Dehydration of the molybdenum trioxide hydrates  $\text{MoO}_3 \cdot n\text{H}_2\text{O}$ : In situ x-ray absorption spectroscopy study at the Mo K edge. *J. Phys.: Condens. Matter* **12**(9), 1959 (2000).
60. V. Augustyn and B. Dunn: Vanadium oxide aerogels: Nanostructured materials for enhanced energy storage. *C. R. Chim.* **13**(1–2), 130 (2010).
61. O. Ghodbane, J-L. Pascal, and F. Favier: Microstructural effects on charge-storage properties in  $\text{MnO}_2$ -based electrochemical supercapacitors. *ACS Appl. Mater. Interfaces* **1**(5), 1130 (2009).
62. B. Yebka, C. Julien, and G.A. Nazri: Electrochemical behavior of hydrated molybdenum oxides in rechargeable lithium batteries. *Ionics* **5**(3–4), 236 (1999).
63. N. Kumagai, N. Kumagai, and K. Tanno: Electrochemical characteristics and structural changes of molybdenum trioxide hydrates as cathode materials for lithium batteries. *J. Appl. Electrochem.* **18**(6), 857 (1988).
64. D. Muñoz-Santiburcio, C. Wittekindt, and D. Marx: Nanoconfinement effects on hydrated excess protons in layered materials. *Nat. Commun.* **4**, 2349 (2013).
65. M. Winter and R.J. Brodd: What are batteries, fuel cells, and supercapacitors? *Chem. Rev.* **104**(10), 4245 (2004).
66. H. Lin, F. Zhou, C-P. Liu, and V. Ozolins: Non-Grotthuss proton diffusion mechanism in tungsten oxide dihydrate from first-principles calculations. *J. Mater. Chem. A* **2**, 12280 (2014).
67. J.D.E. McIntyre, S. Basu, W.F. Peck, W.L. Brown, and W.M. Augustyniak: Cation insertion reactions of electrochromic tungsten and iridium oxide films. *Phys. Rev. B* **25**(12), 7242 (1982).
68. Y.M. Li, M. Hibino, M. Miyayama, and T. Kudo: Proton conductivity of tungsten trioxide hydrates at intermediate temperature. *Solid State Ionics* **134**(3–4), 271 (2000).
69. M. Walter, K.V. Kravchyk, M. Ibáñez, and M.V. Kovalenko: Efficient and inexpensive sodium–magnesium hybrid battery. *Chem. Mater.* **27**, 7452 (2015).
70. E. Levi, M.D. Levi, O. Chasid, and D. Aurbach: A review on the problems of the solid state ions diffusion in cathodes for rechargeable Mg batteries. *J. Electroceram.* **22**, 13 (2009).
71. S.H. Lapidus, N.N. Rajput, X. Qu, K.W. Chapman, K.A. Persson, and P.J. Chupas: Solvation structure and energetics of electrolytes for multivalent energy storage. *Phys. Chem. Chem. Phys.* **16**(40), 21941 (2014).
72. E. Levi, Y. Gofer, and D. Aurbach: On the way to rechargeable Mg batteries: The challenge of new cathode materials. *Chem. Mater.* **22**(3), 860 (2010).
73. F. Chaput, B. Dunn, P. Fuqua, and K. Salloux: Synthesis and characterization of vanadium oxide aerogels. *J. Non-Cryst. Solids* **188**, 11 (1995).
74. D.B. Le, S. Passerini, J. Guo, J. Ressler, B.B. Owens, and W.H. Smyrl: High surface area  $\text{V}_2\text{O}_5$  aerogel intercalation electrodes. *J. Electrochem. Soc.* **143**(7), 2099 (1996).
75. V. Petkov, P.N. Trikalitis, E.S. Bozin, S.J.L. Billinge, T. Vogt, and M.G. Kanatzidis: Structure of  $\text{V}_2\text{O}_5 \cdot n\text{H}_2\text{O}$  xerogel solved by the atomic pair distribution function technique. *J. Am. Chem. Soc.* **124**(34), 10157 (2002).
76. P.E. Tang, J.S. Sakamoto, E. Baudrin, and B. Dunn:  $\text{V}_2\text{O}_5$  aerogel as a versatile host for metal ions. *J. Non-Cryst. Solids* **350**, 67 (2004).
77. D.B. Le, S. Passerini, F. Coustier, J. Guo, T. Soderstrom, B.B. Owens, and W.H. Smyrl: Intercalation of polyvalent cations into  $\text{V}_2\text{O}_5$  aerogels. *Chem. Mater.* **10**(3), 682 (1998).
78. P. Novák, W. Scheifele, F. Joho, and O. Haas: Electrochemical insertion of magnesium into hydrated vanadium bronzes. *J. Electrochem. Soc.* **142**(8), 2544 (1995).

79. L.W. Wangoh, Y. Huang, R.L. Jezorek, A.B. Kehoe, G.W. Watson, F. Omenya, N.F. Quackenbush, N.A. Chernova, M.S. Whittingham, and L.F.J. Piper: Correlating lithium hydroxyl accumulation with capacity retention in  $V_2O_5$  aerogel cathodes. *ACS Appl. Mater. Interfaces* **8**, 11532 (2016).
80. R. Schöllhorn: In *Intercalation Chemistry*, M.S. Whittingham and A.J. Jacobson eds.; Academic Press: New York, 1982; pp. 315–360.
81. G. Sai Gautam, P. Canepa, W.D. Richards, R. Malik, and G. Ceder: Role of structural  $H_2O$  in intercalation electrodes: The case of Mg in nanocrystalline xerogel- $V_2O_5$ . *Nano Lett.* **16**, 2426 (2016).
82. J. Song, M. Noked, E. Gillette, J. Duay, G. Rubloff, and S.B. Lee: Activation of a  $MnO_2$  cathode by water-stimulated  $Mg^{2+}$  insertion for a magnesium ion battery. *Phys. Chem. Chem. Phys.* **17**(7), 5256 (2015).
83. X. Sun, V. Duffort, B.L. Mehdi, N.D. Browning, and L.F. Nazar: Investigation of the mechanism of Mg insertion in birnessite in non-aqueous and aqueous rechargeable Mg-ion batteries. *Chem. Mater.* **28**, 534 (2015).
84. J.R. González, F. Nacimiento, M. Cabello, R. Alcántara, P. Lavela, and J.L. Tirado: Reversible intercalation of aluminium into vanadium pentoxide xerogel for aqueous rechargeable batteries. *RSC Adv.* **6**(67), 62157 (2016).
85. A.M. Chippendale and A.K. Cheetham: In *Molybdenum: An Outline of its Chemistry and Uses*, E.R. Braithwaite and J. Haber, eds. (Elsevier, Amsterdam, 1994); pp. 146–184.
86. H. Tagaya, K. Ara, J. Kadokawa, M. Karasu, and K. Chiba: Intercalation of organic compounds in the layered host lattice  $MoO_3$ . *J. Mater. Chem.* **4**(4), 551 (1994).
87. D. Chen, M. Liu, L. Yin, T. Li, Z. Yang, X. Li, B. Fan, H. Wang, R. Zhang, Z. Li, H. Xu, H. Lu, D. Yang, J. Sun, and L. Gao: Single-crystalline  $MoO_3$  nanoplates: Topochemical synthesis and enhanced ethanol-sensing performance. *J. Mater. Chem.* **21**(25), 9332 (2011).
88. J.B. Rivest and P.K. Jain: Cation exchange on the nanoscale: An emerging technique for new material synthesis, device fabrication, and chemical sensing. *Chem. Soc. Rev.* **42**(1), 89 (2013).
89. A. Manthiram: In *Lithium Batteries: Science and Technology*, G.A. Nazri and G. Pistoia eds.; Springer, New York, 2003; pp. 3–41.
90. D. Larcher, M.R. Palacín, G.G. Amatucci, and J.-M. Tarascon: Electrochemically active  $LiCoO_2$  and  $LiNiO_2$  made by cationic exchange under hydrothermal conditions. *J. Electrochem. Soc.* **144**(2), 408 (1997).
91. W. Liu, P. Oh, X. Liu, M.-J. Lee, W. Cho, S. Chae, Y. Kim, and J. Cho: Nickel-rich layered lithium transitional-metal oxide for high-energy lithium-ion batteries. *Angew. Chem., Int. Ed.* **54**, 4440 (2015).
92. R.A. Armstrong, P.G. Bruce, A.R. Armstrong, and P.G. Bruce: Synthesis of layered  $LiMnO_2$  as an electrode for rechargeable lithium batteries. *Nature* **381**, 499 (1996).
93. F. Capitaine, P. Gravereau, and C. Delmas: A new variety of  $LiMnO_2$  with a layered structure. *Solid State Ionics* **89**, 197 (1996).
94. T.E. Quine, M.J. Duncan, A.R. Armstrong, A.D. Robertson, and P.G. Bruce: Layered  $Li_xMn_{1-x}Ni_xO_2$  intercalation electrodes. *J. Mater. Chem.* **10**(12), 2838 (2000).
95. B.E. Ruiz-hitzky and E. Ruiz-Hitzky: Conducting polymers intercalated in layered solids. *Adv. Mater.* **5**, 334 (1993).
96. Y. Chen, G. Yang, Z. Zhang, X. Yang, W. Hou, and J.-J. Zhu: Polyaniline-intercalated layered vanadium oxide nanocomposites—one-pot hydrothermal synthesis and application in lithium battery. *Nanoscale* **2**(10), 2131 (2010).
97. M. Malta and R.M. Torresi: Electrochemical and kinetic studies of lithium intercalation in composite nanofibers of vanadium oxide/polyaniline. *Electrochim. Acta* **50**, 5009 (2005).
98. L. Peng, Y. Zhu, D. Chen, R.S. Ruoff, and G. Yu: Two-dimensional materials for beyond-lithium-ion batteries. *Adv. Energy Mater.* **6**, 1600025 (2016).
99. J. Liu and X.-W. Liu: Two-dimensional nanoarchitectures for lithium storage. *Adv. Mater.* **24**(30), 4097 (2012).
100. K. Kalantar-Zadeh, A. Vijayaraghavan, M.H. Ham, H. Zheng, M. Breedon, and M.S. Strano: Synthesis of atomically thin  $WO_3$  sheets from hydrated tungsten trioxide. *Chem. Mater.* **22**(19), 5660 (2010).
101. H. Zhang, L. Gao, and Y. Gong: Exfoliated  $MoO_3$  nanosheets for high-capacity lithium storage. *Electrochem. Commun.* **52**, 67 (2015).
102. Q. Du, M. Zheng, L. Zhang, Y. Wang, J. Chen, L. Xue, W. Dai, G. Ji, and J. Cao: Preparation of functionalized graphene sheets by a low-temperature thermal exfoliation approach and their electrochemical supercapacitive behaviors. *Electrochim. Acta* **55**(12), 3897 (2010).
103. M. Aksit, D.P. Toledo, and R.D. Robinson: Scalable nanomanufacturing of millimetre-length 2D  $Na_xCoO_2$  nanosheets. *J. Mater. Chem.* **22**(13), 5936 (2012).
104. R. Ma and T. Sasaki: Two-dimensional oxide and hydroxide nanosheets: Controllable high-quality exfoliation, molecular assembly, and exploration of functionality. *Acc. Chem. Res.* **48**, 136 (2014).
105. D. Hanlon, C. Backes, T.M. Higgins, M. Hughes, A. O'Neill, P. King, N. McEvoy, G.S. Duesberg, B. Mendoza Sanchez, H. Pettersson, V. Nicolosi, and J.N. Coleman: Production of molybdenum trioxide nanosheets by liquid exfoliation and their application in high-performance supercapacitors. *Chem. Mater.* **26**(4), 1751 (2014).
106. Y. Li, X. Shi, X. Lang, Z. Wen, J. Li, and Q. Jiang: Remarkable improvements in volumetric energy and power of 3D  $MnO_2$  microsupercapacitors by tuning crystallographic structures. *Adv. Funct. Mater.* **26**, 1830–1839 (2016).
107. Q. Cheng, T. Yang, Y. Li, M. Li, and C.K. Chan: Oxidation–reduction assisted exfoliation of  $LiCoO_2$  into nanosheets and reassembly into functional Li-ion battery cathodes. *J. Mater. Chem. A* **4**, 6902 (2016).
108. A.K. Geim and I.V. Grigorieva: Van der Waals heterostructures. *Nature* **499**(7459), 419 (2013).
109. B. Mendoza-Sánchez, J. Coelho, A. Pokle, and V. Nicolosi: A 2D graphene-manganese oxide nanosheet hybrid synthesized by a single step liquid-phase co-exfoliation method for supercapacitor applications. *Electrochim. Acta* **174**, 696 (2015).
110. D. Wang, R. Kou, D. Choi, Z. Yang, Z. Nie, J. Li, L.V. Saraf, D. Hu, J. Zhang, G.L. Graff, J. Liu, M.A. Pope, and I.A. Aksay: Ternary self-assembly of ordered metal oxide-graphene nanocomposites for electrochemical energy storage. *ACS Nano* **4**(3), 1587 (2010).
111. Z.-S. Wu, G. Zhou, L.-C. Yin, W. Ren, F. Li, and H.-M. Cheng: Graphene/metal oxide composite electrode materials for energy storage. *Nano Energy* **1**(1), 107 (2012).
112. M.S. Whittingham: Electrical energy storage and intercalation chemistry. *Science* **192**(4244), 1126 (1976).
113. K. Mizushima, P.C. Jones, P.J. Wiseman, and J.B. Goodenough:  $Li_xCoO_2$  ( $0 < x < 1$ ): A new cathode material for batteries of high energy density. *Mater. Res. Bull.* **15**, 783 (1980).
114. D. Kim, S.H. Kang, M. Slater, S. Rood, J.T. Vaughey, N. Karan, M. Balasubramanian, and C.S. Johnson: Enabling sodium batteries using lithium-substituted sodium layered transition metal oxide cathodes. *Adv. Energy Mater.* **1**(3), 333 (2011).
115. G. Singh, N. Tapia-ruiz, J. Miguel, U. Maitra, W. James, A.R. Armstrong, J.M. De Ilarduya, T. Rojo, P.G. Bruce, G. Singh, N. Tapia-ruiz, J. Miguel, U. Maitra, J.W. So, A.R. Armstrong, J.M. De Ilarduya, T. Rojo, and P.G. Bruce: High voltage Mg-doped  $Na_{0.67}Ni_{0.3-x}Mg_xMn_{0.7}O_2$  ( $x = 0.05, 0.1$ ) Na-ion cathodes with enhanced stability and rate capability. *Chem. Mater.* **28**, 5087–5094 (2016).